Relative contributions of climate change, stomatal closure, and leaf area index changes to 20th and 21st century runoff change: A modelling approach using the Organizing Carbon and Hydrology in Dynamic Ecosystems (ORCHIDEE) land surface model

Ramdane Alkama, Masa Kageyama, Gilles Ramstein

JOURNAL OF GEOPHYSICAL RESEARCH, VOL. 115, D17112, doi:10.1029/2009JD013408, 2010

Relative contributions of climate change, stomatal closure, and leaf area index changes to 20th and 21st century runoff change: A modelling approach using the Organizing Carbon and Hydrology in Dynamic Ecosystems (ORCHIDEE) land surface model

Ramdane Alkama,[1] Masa Kageyama,[2] and Gilles Ramstein[2]

Received 19 October 2009; revised 30 April 2010; accepted 3 May 2010; published 9 September 2010.

[1] The recent evolution of continental runoff is still an open question. A related and controversial question is the attribution of this change and its consequences on our predictions of the behavior of future runoff. Here, the Land Surface Model Organizing Carbon and Hydrology in Dynamic Ecosystems is used to perform a set of transient simulations of the runoff from 1900 to 2100. We first show that the model's simulated runoff increases for the 20th century from a global point of view as well as its geographical pattern changes are close to the observations made in this paper. Moreover this trend is simulated to increase further during the 21st century under the SRES A2 scenario. We have designed a set of simulations to test the impact on global runoff evolution of three factors: climate, stomatal conductance, and vegetation growth, all sensitive to CO_2 increase. A complete factor-separation analysis of the influence of these three factors and of their interactions shows that climate change largely drives the 20th and 21st century runoff increase. The other two factors (stomatal conductance and vegetation growth) play a minor role in the 20th century runoff trend but we show that these contributions increase for the 21st century simulations. Although the interactions between the factors also plays a negligible role in the 20th century global runoff increase, our results show that they become significant during the 21st century, usually reducing the direct effect of each factor. However, our study does not reveal any important negative feedback to counteract the effect of climate warming on the hydrological cycle.

Citation: Alkama, R., M. Kageyama, and G. Ramstein (2010), Relative contributions of climate change, stomatal closure, and leaf area index changes to 20th and 21st century runoff change: A modelling approach using the Organizing Carbon and Hydrology in Dynamic Ecosystems (ORCHIDEE) land surface model, *J. Geophys. Res.*, *115*, D17112, doi:10.1029/2009JD013408.

1. Introduction

[2] Climate change due to human activity is expected to alter the global hydrological cycle over the next centuries [*IPCC*, 2007]. A growing amount of evidence shows that global runoff has already increased significantly since the beginning of the 20th century [*Labat et al.*, 2004; *Garcia and Mechoso*, 2006; *Peterson et al.*, 2002]. But did runoff really increase since 1950? For the most recent observational study [*Dai et al.*, 2009], the answer is still very uncertain (Figure 1). It is also difficult to define whether such a trend is caused by natural variability or by human factors. Indeed, the physical and dynamical properties of the water cycle depend on many interrelated links between climate, soil, and vegetation dynamics at the continental scale. Overall, long-term changes in runoff depend on the balance of continental precipitation and evapotranspiration. The latter is not only driven by climate factors (e.g., precipitation, temperature, wind speed, humidity, and solar radiation), but also modulated by vegetation growth conditions, themselves sensitive to atmospheric CO_2 variations and climate [*Betts et al.*, 1997]. In summary, an increased atmospheric CO_2 can produce an influence on the river runoff via the following three main mechanisms:

[3] (1) The precipitation increase over land due to the increased evaporation over the oceans related to surface warming [*Labat et al.*, 2004]. Climate change can also cause decreases in runoff via decreasing precipitation in some regions. On the other hand, temperature, wind speed, and humidity, also have an impact on land evapotranspiration. For example, runoff can be affected by the increased evaporative demand over land due to increased temperature. We define all these effects as "climate change" effects.

[4] (2) The decreased transpiration due to the closure of the leaf stomata induced by increased CO_2. Indeed, plants

[1]CNRS/Météo-France, GAME/CNRM, Toulouse, France.
[2]Laboratoire des Sciences du Climat et de l'Environnement/IPSL UMR 8212 CEA, CNRS, l'Université de Versailles Saint-Quentin, Gif sur Yvette, France.

0148-0227/10/2009JD013408

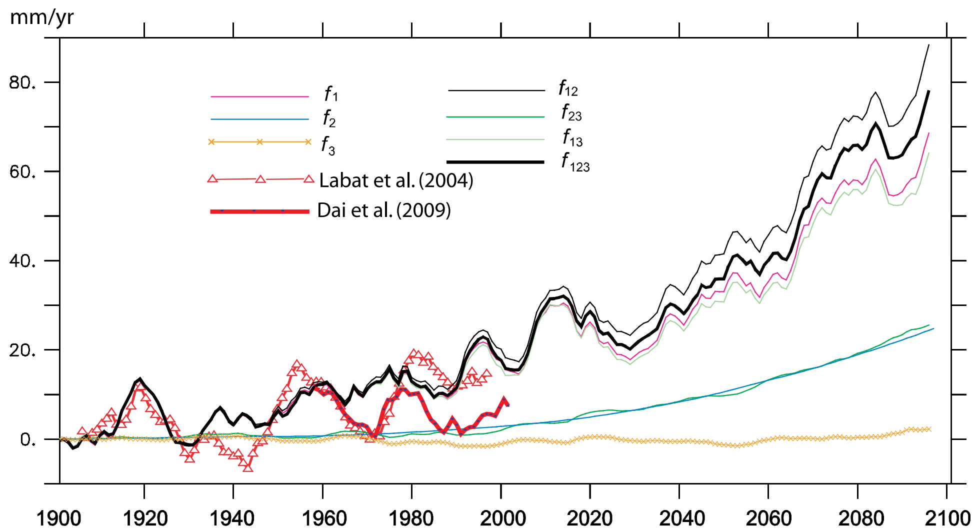

Figure 1. Global runoff evolution from years 1900 to 2100, in anomalies compared to 1900, for the seven different simulations. The observed runoff anomaly is from *Labat et al.* [2004] for the 1900–1994 period and *Dai et al.* [2009] for the 1950–2004 period. There is a net spreading after 2020 that increases until 2100.

regulate the opening and closing of their stomata in response to changing environmental conditions: In a high-CO_2 atmosphere, their stomata do not open as much or for as long, and, therefore, less water is lost from leaves to the atmosphere [*Field et al.*, 1995]. As a consequence, plants acquire enough carbon through their stomata with less water uptake from the soil: They are more efficient in their use of soil moisture. The result is that continental evapotranspiration is reduced [*Betts et al.*, 1997], more moisture is left in the soil, and this additional surface water can lead to increased continental runoff [*Gedney et al.*, 2006]. In the rest of the text, we define this effect as the "CO_2-induced stomatal closure" effect;

[5] (3) CO_2 increase leads to increased vegetation growth, measured for instance by the leaf area index (LAI), and therefore to an increased evapotranspiration [*Betts et al.*, 1997, 2006; *Cramer et al.*, 2001; *Levis et al.*, 2000]. This reduces soil moisture and consequently causes the runoff to decrease. In the literature, this effect is defined as the "CO_2 fertilization' effect. But vegetation growth can also be sensitive to climate change. For example, a decrease in precipitation can induce an LAI decrease due to water limitation. In contrast, increasing precipitation leads to increased vegetation growth. Also, temperature, humidity and wind speed can clearly have an effect on the vegetation growth (and hence on the LAI) and consequently on runoff. We define this vegetation growth effect as the "LAI" effect.

[6] Using the MOSES Land Surface Model, *Gedney et al.* [2006] suggest that the increase of atmospheric CO_2 during the 1960–1994 period is responsible for an increase of global runoff through the stomatal closure effect. However, they do not consider the LAI effect. Using the same model and taking this effect into account, *Betts et al.* [2007] extend the work of *Gedney et al.* [2006] and conclude that the stomatal closure effect is also a major player in explaining the runoff trend for an atmospheric CO_2 doubling. In one of their simulations, they estimate the LAI impact to be negligible. The main reason for LAI effects being negligible at the global scale was the reduced LAI in South America associated with the "Amazon die-back" characteristic of the Hadley Center models. In contrast, using the ORCHIDEE model, *Piao et al.* [2007] suggest that the 20th century fertilization effect overcompensates the stomatal conductance effect but still remains negligible compared to the climate and land use effects.

[7] This difference between the results of *Gedney et al.* [2006] and of *Piao et al.* [2007] can either be attributed to the difference in the physics used in each model or to the methodology used to quantify the impact of each factor in these two studies. Indeed, to isolate the various effects *Gedney et al.* [2006] carry out five simulations. They allow all factors likely to affect runoff (climate, aerosol concentration, atmospheric CO_2, and land use) to vary throughout the fully transient first simulation. In the other four simulations, they allow three of the four factors to vary while they fix the other component to initial conditions. The impact of each individual component is then calculated by comparing the fixed-component simulations with the first "all" simulation. In a different way, *Piao et al.* [2007] carried out three simulations (varying only atmospheric CO_2 in the first simulation, varying both atmospheric CO_2 and climate in the second simulation, and finally varying both atmospheric CO_2, climate and land use in the third simulation). The impact of atmospheric CO_2 component is directly derived from the first simulation, the climate factor is quantified by the second minus first experiment, and finally the land use effect is derived from third experiment minus the second one.

[8] Here we use the factor separation method [*Stein and Alpert*, 1993] to separate the effect of each of the factors introduced above: (1) climate change, (2) CO_2-induced stomatal closure, and (3) LAI, and of their interactions on the runoff trends over 20th and 21st centuries. To our knowledge, this is the first time that this method is applied to comprehensively analyze the causes of the global runoff evolution for this period. In the first simulation, the ORCHIDEE land surface model [*Krinner et al.*, 2005] is forced with the observed 20th century CO_2 evolution and 21st century IPCC A2 CO_2 scenario and by the corresponding climate evolution simulated by the IPSL coupled ocean atmosphere model

[*Marti et al.*, 2010]. We first validate the results using data from the 20th century, then we attribute the runoff trend over 20th and 21st centuries and analyze the differences between these two periods. The factor-separation methodology requires a set of seven transient simulations to fully distinguish the impact of the individual factors and of their interactions. These are needed to quantify each term of equation (1). The seven simulations are carried out with the ORCHIDEE model run offline. Simulation f_{123}, taking all factors into account, is run first. In the other six simulations, the factors are either kept at their initial state or taken to vary exactly as in the f_{123} simulation, so that their impact and the impact of their interactions can be analyzed according to the factor separation technique [*Stein and Alpert*, 1993]. The experiments are designed as follows:

[9] • $\boldsymbol{f_{123}}$ ("all factors") is a control simulation in which CO_2 and climate vary according to the scenarios presented above and in which LAI is allowed to change in response to CO_2 and climate;

[10] • $\boldsymbol{f_1}$ ("climate change effect") is a simulation forced by the climate change scenario only with LAI and CO_2 fixed at their preindustrial value (286.2 ppm for the CO_2 concentration);

[11] • $\boldsymbol{f_2}$ ("CO_2-induced stomatal closure effects") is a simulation in which only CO_2 changes, and in which a repetition of the 1860 climate is used as climate forcing all along the simulation. The LAI is fixed to its preindustrial value;

[12] • $\boldsymbol{f_3}$ ("LAI effect") is a simulation in which only LAI changes ($\boldsymbol{f_3}$), using the LAI simulated in the control (f_{123}) simulation. The climate and CO_2 forcings are taken to their 1860 values;

[13] • $\boldsymbol{f_{12}}$ ("climate change and CO_2-induced stomatal closure [at fixed LAI] effects") is a simulation in which the LAI is fixed to its preindustrial value and both climate and CO_2 vary as in the f_{123} simulation;

[14] • $\boldsymbol{f_{13}}$ ("climate change and LAI effects") is a simulation in which CO_2 is fixed to its 1860 value and in which the climate and LAI forcings are the same as in the f_{123} simulation;

[15] • $\boldsymbol{f_{23}}$ ("CO_2-induced stomatal closure and LAI effects") is a simulation in which climate is fixed to its 1860 value and CO_2 and LAI vary as in the $\boldsymbol{f_{123}}$ experiment.

[16] Following *Stein and Alpert* [1993], with the seven experiments defined above, the total impact of the three factors can be decomposed as:

$$f_{123} = f_1 + f_2 + f_3 + f^{12} + f^{13} + f^{23} + f^{123} \tag{1}$$

with

$$f^{12} = f_{12} - f_1 - f_2 \tag{2}$$

$$f^{13} = f_{13} - f_1 - f_3 \tag{3}$$

$$f^{23} = f_{23} - f_2 - f_3 \tag{4}$$

where: f^{12} is representative of the interactions between the impacts of climate change and of CO_2 on stomatal closure effects (role of temperature and humidity on the stomata opening), f^{13} is representative of the interactions between the climate change and LAI effects, f^{23} is representative of the interactions between the impact of CO_2 on stomatal closure and LAI effects, and finally f^{123} is representative of the interactions between the effects of climate change, the impact of CO_2 on stomatal closure and LAI on the global river runoff. This comprehensive set of experiments allows the analysis of all forcing factors and associated feedbacks.

[17] In the f_2, f_3, and f_{23} simulations, we use the repetition of the 1860 preindustrial climate defined as the average of last 50 years of a 300 year long simulation using the IPSL_CM4 coupled ocean-atmosphere general circulation model with preindustrial boundary conditions. It would be difficult to separate the impacts of the LAI or the stomatal conductance effect on the runoff change if we use a repetition of 20–30 years from this simulation, because the climate interannual variability can interact differently under 1900 or 2100 LAI conditions. For this reason, we prefer to use a repetition of an averaged 50 preindustrial climate. Also, even if the CO_2 in f_2 is the same as in f_{123}, the stomatal conductance effect in f_2 is different from that simulated in f_{123}. Indeed, temperature and humidity also play a role in the stomata opening (this can estimated as the interaction between CO_2 and climate change f^{12}). Also, the stomatal conductance effect on the land runoff depends on the LAI effects (this also can be estimated as interaction between CO_2 and LAI f^{23}).

[18] In this work, we have not included experiments to isolate the impact of land use changes. The impact of land use change on river runoff via evapotranspiration change is still unclear. Indeed, when irrigation is neglected, land use could play an important role on the global river runoff increase via a decrease in evapotranspiration [*Piao et al.*, 2007]. On the contrary, studying the Chinese region, *Liu et al.* [2008] demonstrate that deforestation leads on average to increased evapotranspiration for the 20th century, due to the irrigation of the agricultural land replacing the forest. *Sun et al.* [2008] confirm this result for the sub tropical Chinese region for the period 1967–1993. Conversely, over the Mississippi river basin, *Twine et al.* [2004] suggest that deforestation acts to decrease evapotranspiration but that changing grassland to land use acts to increase it. Over Tocantins Basin of the Amazonian region, *Costa et al.* [2003] show an increase in river runoff associated with an increase in agricultural land and no precipitation change. Finally, using two different models, *VanShaar et al.* [2002] show that the impact of land use on the Columbia River hydrology is model dependent. We consider the impact of this factor to be a complex problem beyond the scope of this paper. Furthermore, it is more difficult to develop the methodology we use in this context, all the more difficult that we would have to rely on land use and associated irrigation change scenarios for the 21st century, for which the uncertainty is larger than for the physical factors analyzed in our study. For all these reasons, we limit our analysis to the three physical factors described above.

2. Results

2.1. The 20th Century Runoff Evolution

[19] The simulated evolution of global mean runoff in the 20th century, taking into account the combined effects of changes in climate, CO_2-induced stomatal closure, and LAI (simulation f_{123}) (Figure 1) is characterised by a significant positive trend of 0.19 mm yr^{-2}. This simulated trend is in good argument with the observed trend [*Labat et al.*, 2004] of

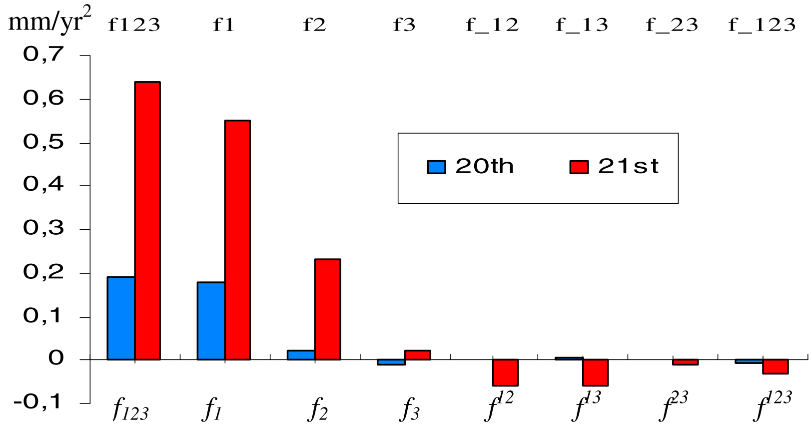

Figure 2. Global runoff trends over the 20th century (blue) and 21st century (red) due to different factors and their interactions (mm yr^{-2}). Using factor analysis method such plots are easy to provide for different climate simulations and should facilitate intercomparison.

0.18 mm yr^{-2}. In contrast, the newer estimation of the global land runoff trend over 1950–2004 [*Dai et al.*, 2009] shows a slight negative trend −0.05 mm yr^{-2}. For the same period, the f_{123} simulation exhibits a large positive trend 0.27 mm yr^{-2}. Our set of simulations demonstrates that both the trend in global runoff and the fluctuations around this trend can be primarily attributed to the prescribed climate evolution. Indeed all simulations including the climate change forcing (f_1, f_{12}, and f_{13}) show a behavior similar to the simulation including all factors (f_{123}), which is not the case for the simulations that do not include the climate forcing (f_2, f_3, and f_{23}). The estimated evolution of global runoff induced by climate change only (f_1) is 0.18 mm yr^{-2}, which represents 95% of the global simulated trend for the 20th century. On the other hand, the 70 ppmv increase in atmospheric CO_2 concentration between 1901 and 2000 produces a significant rise of global runoff via the stomatal closure effect (f_2), since it reaches an annual increase of 0.02 mm yr^{-2}, i.e., 10% of the global simulated trend. Conversely, the impact of the LAI change (f_3) corresponds to a decrease in global runoff of 0.01 mm yr^{-2}. Therefore, the impact of CO_2 on stomatal closure and LAI changes related to CO_2 increase, on global runoff, as well as the interactions between the two of these factors, remain weak compared to the direct effect of climate evolution for the 20th century (Figures 1 and 2).

[20] Despite its global average significant increase, runoff exhibits a pronounced geographical heterogeneity in its trends (Figure 3a), which mainly results from spatial differences in climatic conditions (Figure 3b). For example, the largest runoff increase tendency (more than 1 mm yr^{-2}) is located in equatorial regions, especially over Indonesia, Malaysia, the western part of the Amazon basin, and equatorial Africa, and also in eastern Canada and the northern part of Europe, where significant increases of annual precipitation occur during the 20th century climate simulation. In contrast, because of a substantial reduction of annual precipitation, the eastern Amazon basin, southern Asia, and the Mediterranean basin undergo a strong negative runoff trend. Similar spatial patterns in runoff trend are also observed in data from the recently compiled runoff observation data [*Milly et al.*, 2005]. Over the 1950–2004 period, comparing the estimated runoff by *Dai et al.* [2009] over the 180 largest river basins (Figure 4a), the f_{123} simulation captures the trend in river runoff over most continents (Figure 4b) except over the southern part of North America, Indochina and the Yellow River, Yangtze River, the Loire and Madagascar rivers for which the observations show a positive trend while the simulations show the opposite. In the opposite way, the Columbia, Fraser, and surrounding rivers in North American, New Guinea, and New Zealand show positive trends in the simulations while it is negative in the reconstructed data by *Dai et al.* [2009]. Over some regions like the southern part of North America for instance, the simulated runoff change can be improved when using the CRU observed climate forcing and CO_2 (both the CO_2-induced stomatal closure and the LAI effect are taken into account in this simulation) during the 1950–2004 period (Figure 4c). In contrast, principally over high-latitude boreal regions, the simulated runoff trend is closer to the reconstructions when using the IPSL simulated climate (f_{123}) forcing (Figure 4b). Over boreal regions, especially over Siberia, the IPSL model simulates a positive precipitation trend in line with observed runoff but in contrast with the CRU observed precipitations. On the one hand, the quality of the observed precipitation, which is based on a limited number of in situ rain gauges over Siberia, may not be sufficient to reproduce the observed runoff trend. On the other hand, the fact that the increasing trends in streamflow are not associated with increasing precipitation can suggest that the recent surface warming and associated decline of permafrost and glaciers, not yet included in the ORCHIDEE model, could have contributed to increased runoff at high latitude (Alkama R., B. Decharme, H. Douville, and A. Ribes, Global runoff trends over recent decades: Methodological issues and sources of uncertainty. *Journal of Climate*, submitted). Therefore, our simulations not only reproduce the global trend in runoff during 20th century, but also most of its geographical pattern. For both, we show that these variations are mainly climate driven. What about the next century?

2.2. The 21st Century

[21] The increase in annual runoff simulated for the 21st century (0.64 mm yr^{-2}) under the SRES A2 scenario is three times as large as the one obtained for the 20th century (0.19 mm yr^{-2}). As for the 20th century, the first-order impact

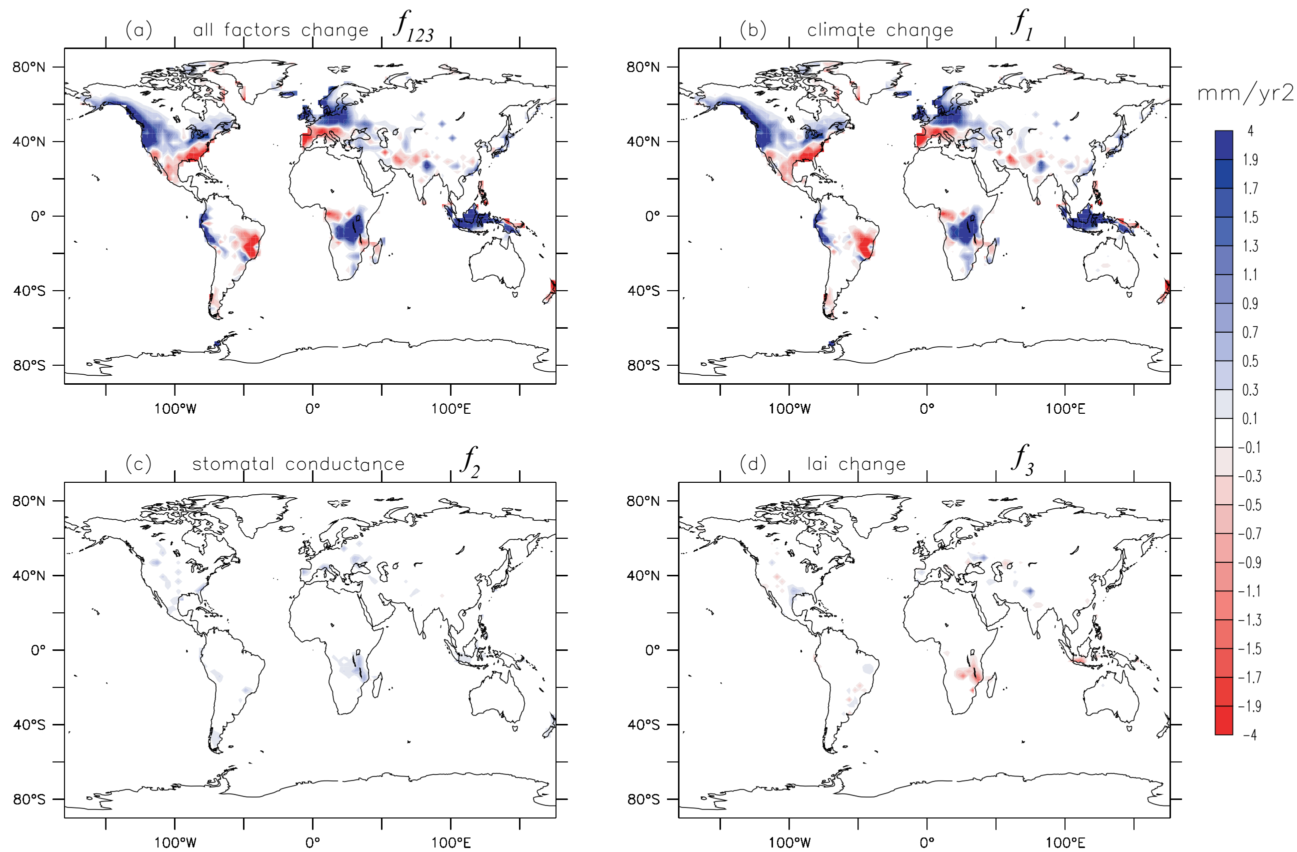

Figure 3. Spatial distribution of the trend in modeled runoff during the 20th century due to all factors (f_{123}) and to each factor taken separately (f_1, climate change; f_2, CO_2 induced stomatal closure; f_3, LAI). The impact of the interactions between the different factors is negligible (compare Figure 5) and are therefore not shown.

of CO_2 increase on global runoff is again driven by the climate response to this increase, i.e., by the associated increased temperature and moisture. Indeed, the climate change effect (simulation f_1) represents 86% (0.55 mm yr^{-2}) of the annual runoff increase (Figures 1 and 2). The contribution of CO_2-induced stomatal conductance change considered separately from the other factors (f_2) reaches around a third (0.23mm yr^{-2}) of the total mean trend and therefore corresponds to a much larger contribution than for the 20th century. More than 50% of the runoff increase due to this factor takes place over equatorial and tropical regions located south of 5°N (Figures 5c and 2), as expected from the LAI geographical distribution (high-LAI regions imply more stomata and a greater influence of this factor). The LAI impact (f_3) consists of a slight increase in the runoff trend (0.02mm yr^{-2}), which corresponds to only 3% of the total mean trend. Interestingly, this trend is opposite to the one simulated for the 20th century. This is due to the fact that in the f_{123} simulation, from which the LAI is taken as a forcing for simulation f_3, global LAI increases due to climate change and CO_2 increase in the 20th and 21st centuries, but it decreases over large areas, such as southern North America and the Mediterranean Basin, during the 21st century, especially after 2050, as a result of climate changes (not shown). Even if global mean LAI increases in the f_3 simulation, runoff increases much more over the regions where the LAI decreases than over regions where it increases (Figure 5d). This is essentially due to the water limitation over the latter areas. Indeed, the preindustrial precipitation (which is the forcing used in the f_3 simulation) over the regions where LAI increases is too low to obtain a significant increase in evapotranspiration. In contrast, in regions where LAI decreases, the preindustrial precipitation is favorable to runoff increase.

[22] As for the 20th century, the significant increase of global average runoff masks a pronounced geographical heterogeneity (Figure 5a), which again mainly results from the heterogeneities in the changes in climatic conditions (Figure 5b). For example, the largest increase in runoff (over more than 1 mm yr^{-2}) is located North of 45°N and in equatorial regions (25°S–5°N) such as Indonesia, Malaysia, the Amazon Basin, where strong increases of annual precipitation are predicted by the IPSL model. On the other hand, a decline of precipitation occurs over southern North America and the Mediterranean basin (5°N–40°N latitude band on Figure 5b) and explains the runoff decrease over these regions. Similar spatial patterns of precipitation changes, especially for the continents north of 40°N, have also been simulated with other models in the last IPCC exercise [*IPCC*, 2007].

[23] The plants open and close their stomata in response to changing environmental conditions, such as light intensity, temperature, humidity, and carbon dioxide concentration. According to simulation f_2 (where preindustrial climate and

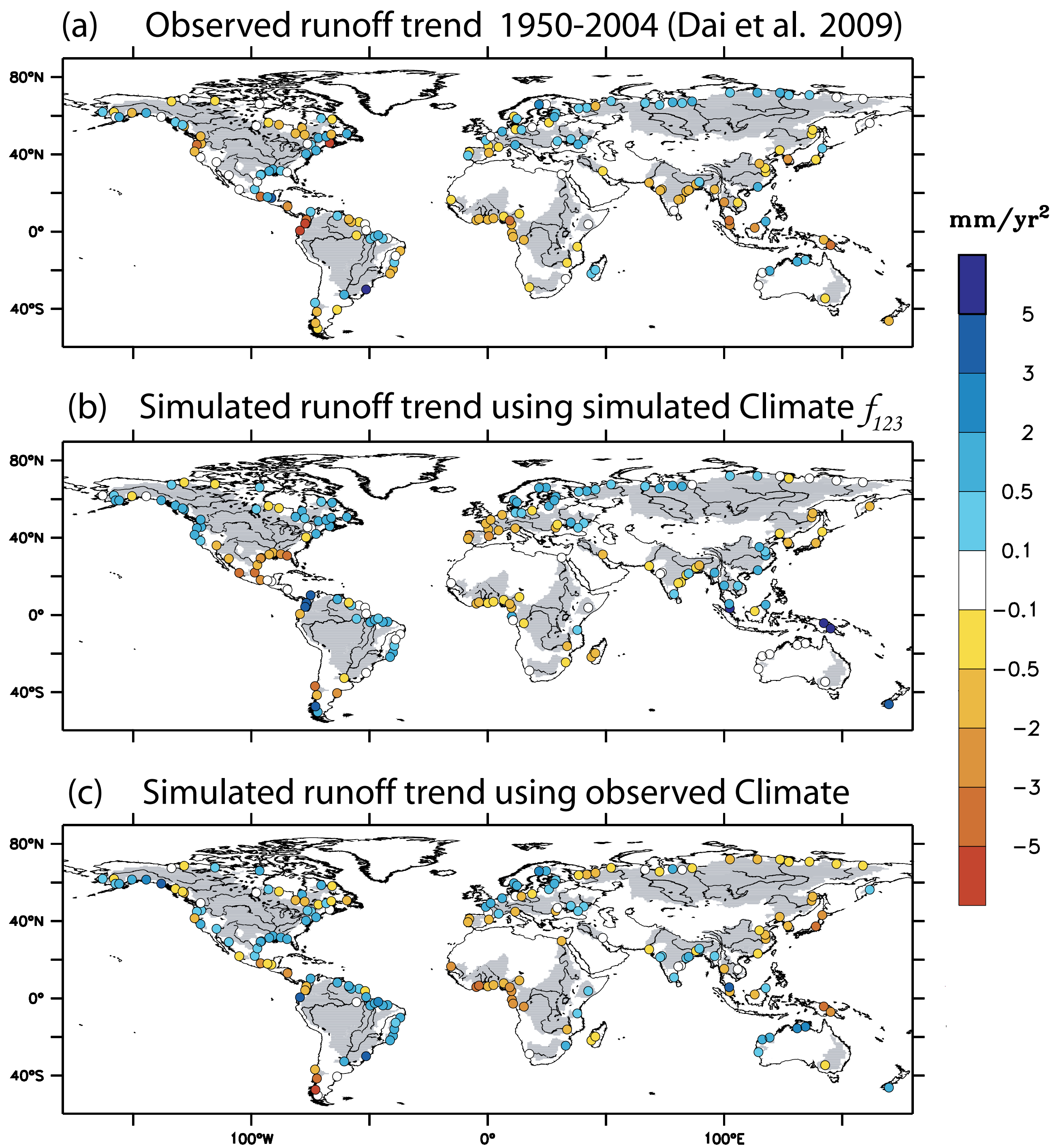

Figure 4. Distribution of the downstream outlets (dots) for the 180 largest rivers included in this study. The drainage area of each basin is given in gray. The color of the dots indicates the observed [*Dai et al.*, 2009] (up), simulated using the IPSL simulated climate (f_{123}, middle) and simulated using CRU observed climate [as in *Piao et al.*, 2007] i.e., both CO_2-induced stomatal closure and LAI effect are taken into account in this simulation but without including land use change, (down) runoff trend (mm yr^{-2}) over 1950–2004 period.

LAI are prescribed during the whole simulation), the CO_2 impact on stomatal closure effect induces a general runoff increase (Figure 5c), especially over the regions where the preindustrial climate (mainly humidity) and initial vegetation are favourable for an impact of the stomatal closure, and very small magnitude over other regions. On the other hand, the temperature and humidity effect on the stomata opening (estimated as the interaction between CO_2 and climate change f^{12}) (Figure 5e) shows decreases in runoff over the regions of maximum runoff increase in f_2, which roughly correspond to the regions where the 21st century shows precipitation decrease compared with the preindustrial climate. In contrast,

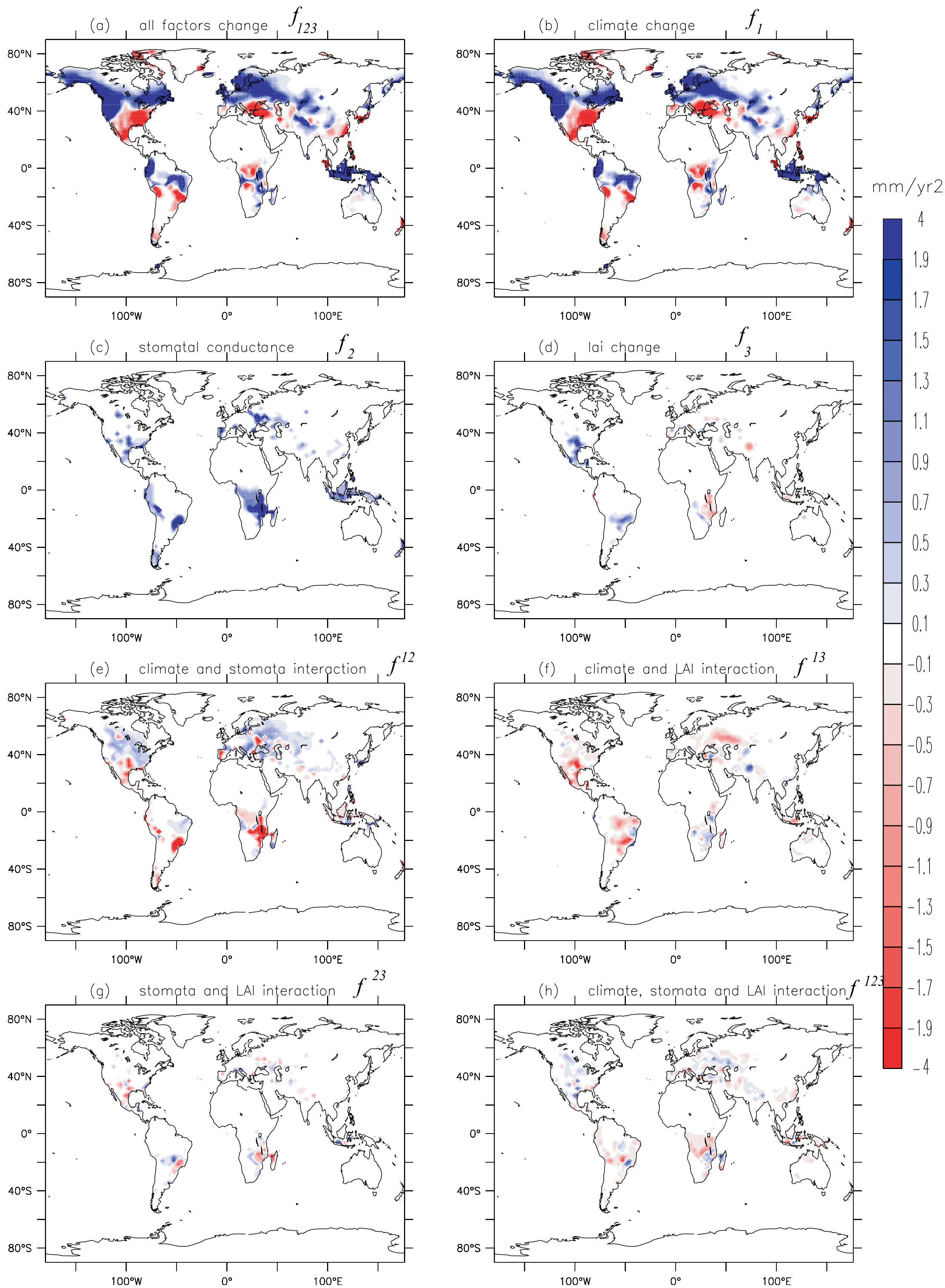

Figure 5. Spatial distribution of the trend in modeled runoff over 21st century due to all factors (f_{123}), to each factor taken separately (f_1, climate change; f_2, CO_2 induced stomatal closure; f_3, LAI) and to the interactions between the different factors.

it increases over other regions, where the 21st century precipitation increases.

[24] With constant preindustrial climate, reduced LAI leads to reduced evapotranspiration (especially over wet regions) and as a result increased runoff. Conversely, increased LAI leads to increased evaporation (in regions where there is enough precipitation) and reduced runoff. Only varying LAI (f_3, Figure 5d) under a fixed preindustrial climate and stomatal closure induces a large runoff increase over the regions where the LAI is decreasing (wet preindustrial region) and a slight decrease over the regions where the LAI is increasing (dry preindustrial region). On the contrary, the interaction between LAI and climate (f^{13}, Figure 5f) shows an opposite trend compared to f_3.

[25] This result illustrates the capacity of factor separation technique to correctly capture the LAI impact on global river runoff. Only allowing the LAI to vary (f_3) yields a slight global runoff increase (0.02 mm yr^{-2}) over the 21st century, while taking the LAI and its interaction with climate change into account ($f_{13} - f_1$) results in a decrease of global river runoff of about 0.04 mm yr^{-2}. This example shows that this method is appropriate not only to attribute the different contributions (f_1, f_2, f_3), but also to understand the interaction between the parameters.

3. Summary and Conclusions

[26] The present study focuses on the hydrological changes during the 20th and 21st centuries as a consequence of CO_2 increase. The following three mechanisms are considered: climate change due to this increase, stomatal closure due to this increase, and vegetation growth (LAI) changes due to both CO_2 and climate changes. Even if they diverge from the reconstructed [*Dai et al.*, 2009] global land runoff trend over the 1950–2004 period, our results are generally consistent with observed regional distribution. Our results agree with the global land runoff trend reconstructed by *Labat et al.* [2004] for the 20th century. Figure 2 summarizes the global trends in runoff for the 20th (in blue) and the 21st (in red) centuries, in the series of simulations accounting for the combined effects of the three factors (simulation f_{123}), the separate trends induced by each one considered on its own (f_1, f_2, f_3), and thanks to our factor analysis, the impact of their interactions (f^{12}, f^{13}, f^{23}, f^{123}). Our study demonstrates that climate change explains most of the runoff trend. Stomatal conductance is the second most important factor for the 21st century (36% of the global mean runoff trend), a role which is much larger than for the 20th century. The other factors play a minor role at the global scale and, for most of the time, at the regional scale. If we accept the small amplifying effect of the climate-LAI interaction for the 20th century, the interactions between the different factors all have a dampening effect on the global runoff trend, especially for the 21st century. Nevertheless, they remain quite weak in amplitude, although they are stronger for the 21st than for the 20th century. Furthermore, these effects are not systematically similar for both periods, as depicted for instance, by the sign difference between f^{12}, f^{23}, and f^{23} for both periods. Therefore the impact of these interactions cannot be ignored and should be accounted for in future work. The methodology we followed here yields a precise evaluation of the respective contributions of each forcing factor to the runoff trend. Moreover it enables a global and regional study of the impact of the interactions between these factors. Some of our results are different from previous studies using different models [*Gedney et al.*, 2006; *Betts et al.*, 2007]. These studies account for different parameters and therefore their results are difficult to compare with our study. On the other hand, we suggest that the factor separation methodology we used in our study can be easily generalized to other models and should help understanding the differences between these results. There is still some debate about the long-term effect of CO_2 increase on photosynthesis and plant growth. The relative importance of the fertilization and stomatal closure effects are still probably very model dependent.

[27] As explained in the introduction, we do not account for the land use effect, which may play an important role. The evaluation of the land use effects on the past and future runoff trends relies on the availability of associated irrigation scenarios for both 20th and 21st century, and it would therefore be very interesting to quantify the runoff trend for each of these scenarios. It would also be interesting to investigate the potential feedback of these runoff trends on the oceanic circulation and on climate. This impact has been shown to be drastic in the past [*Alkama et al.*, 2008] and should be carefully studied for periods when ice sheet melting will largely perturb the hydrological cycle.

4. Methods and Model Descriptions

[28] The model used for this work is the ORganizing Carbon and Hydrology In Dynamic EcosystEms (ORCHIDEE) Global Vegetation Model, which has been developed to assess the transient impacts of climate change on the transfer of water and carbon in the vegetation-soil-atmosphere system [*Krinner et al.*, 2005]. The land-use used is fixed at its present day value for all simulations. The forcing that we have used for our experiments in terms of climate results from two coupled ocean atmosphere climate experiments using the IPSL_CM4 model [*Marti et al.*, 2010]. The atmosphere component of this coupled model is LMDZ.3.3 [*Hourdin et al.*, 2006], with a resolution of 96 × 72 × 19 points in longitude × latitude × altitude. This atmospheric module includes the ORCHIDEE land surface scheme. The ocean module is ORCA2 [*Madec et al.*, 1998], which uses an irregular horizontal grid of 182 × 149 points with a resolution of 2°, refined over key regions such as the North Atlantic and near the equator. This model has 31 depth levels. The sea-ice module is the Louvain Ice Model (LIM) [*Fichefet and Morales Maqueda*, 1997], developed at Louvain-La-Neuve. The coupling of these components is performed using the OASIS (version 3) coupler [*Valcke et al.*, 2004]. The IPSL_CM4 model has been widely used to assess the impacts of transient anthropogenic forcings on the global or regional climate change [*IPCC*, 2007]. The first coupled experiment reproduces the 1900–2000 climate evolution under the historic aerosol and greenhouse gas concentration evolutions [*Rayner et al.*, 2005]. The second experiment covers the 21st century and uses the SRES A2 scenario. We combine these simulations to obtain a 6 hourly forcing for the period of the 20th and 21st centuries. No correction has been applied to the climate model output. This forcing is interpolated into half hourly forcing, which corresponds to the ORCHIDEE time scale. The formulation of stomatal conductance is modeled

following a semiempirical approach [*Ball et al.*, 1987]. It ensures the consistency between the treatment of the hydrological processes, in particular transpiration, and the treatment of stomatal conductance and photosynthesis, both being intimately linked. Vegetation productivity is calculated based on a coupled photosynthesis–water balance scheme. Plant growth based on the net plant carbon gain is allocated to six tissue pools (leaf, root, and wood, as well as reserve and reproductive organs), with a response of the relative investment into above- and below-ground structures, depending on soil temperature and moisture. Therefore, the ecosystem water balance affects plant carbon gain and structure. Leaf phenology and decomposition of litter and soil organic matter depend on temperature and water stress. The surface scheme hydrology is represented by two soil layers [*Ducoudré et al.*, 1993], where the water content of each layer is updated by accounting for inputs from rainfall and snowmelt, which is reduced by interception losses as well as by losses to soil evaporation, transpiration, deep drainage, and surface runoff. Vegetation transpiration depends on the modeled photosynthetic activity and atmospheric vapor-pressure deficit [*Ball et al.*, 1987], and is mediated by soil-water availability. The amount of water intercepted by the foliage is controlled by the incident rainfall and LAI. Soil evaporation is calculated from the relative humidity of the air at the land surface and aerodynamic and soil resistances, where the soil resistance is a function of soil moisture. Surface runoff and drainage are calculated as the excess water above field capacity in both soil layers.

[29] **Acknowledgments.** This work has been supported by the ANR-BLANC CHAMPION with computer time provided by CEA/CCRT. R. Alkama is supported by the CYMENT project of the RTRA STAE Toulouse. The authors wish to thank Pierre Friedlingstein and three anonymous reviewers for their useful comments on this paper.

References

Alkama, R., et al. (2008), Impact of a realistic river routing in coupled ocean-atmosphere simulations of the Last Glacial Maximum climate, *Clim. Dyn.*, *30*, 855–869.

Ball, J., T. Woodrow, and J. Berry (1987), A model predicting stomatal conductance and its contribution to the control of photosynthesis under different environmental conditions, *Prog. Photosynthesis*, *4*, 221–224.

Betts, R. A., et al. (1997), Contrasting physiological and structural vegetation feedbacks in climate change simulations, *Nature*, *387*, 796–799.

Betts, R. A., et al. (2004), The role of ecosystem-atmosphere interactions in simulated Amazonian precipitation decrease and forest dieback under global climate warming, *Theor. Appl. Climatol.*, *78*, 157–175.

Betts, R. A., et al. (2007), Projected increase in continental runoff due to plant responses to increasing carbon dioxide, *Nature*, *448*, 1037–1041.

Costa, M. H., A. Botta, and J. A. Cardille (2003), Effects of large-scale change in land cover on the discharge of the Tocantins River, Amazonia, *J. Hydrol.*, *283*, 206–217.

Cramer, W., et al. (2001), Global response of terrestrial ecosystem structure and function to CO_2 and climate change: results from six dynamic global vegetation models, *Global Change Biol.*, *7*, 357–373.

Dai, A., T. Qian, K. E. Trenberth, and J. D. Milliman (2009), Changes in continental freshwater discharge from 1948–2004, *J. Climate*, *22*, 2773–2791.

Ducoudré, N. I., K. Laval, and A. Perrier (1993), SECHIBA: a new set of parameterizations of the hydrologic exchanges at the land-atmosphere interface within the LMD atmospheric general circulation model, *J. Clim.*, *6*, 248–273.

Fichefet, T., and M. A. Morales Maqueda (1997), Sensitivity of a global sea ice model to the treatment of ice thermodynamics and dynamics, *J. Geophy. Res.*, *102*, 12,609–12,646.

Field, C., R. Jackson, and H. Mooney (1995) Stomatal responses to increased CO_2: Implications from the plant to the global scale, *Plant Cell Environ.*, *18*, 1214–1255.

Garcia, N. O., and C. R. Mechoso (2006), Variability in the discharge of South America rivers and in climate, *Hydrol. Sci. J.*, *50*, 459–478.

Gedney, N., et al. (2006), Detection of a direct carbon dioxide effect in continental river runoff records, *Nature*, *439*, 835–838.

Hourdin, F., et al. (2006), The LMDZ4 general circulation model: climate performance and sensitivity to parameterized physics with emphasis on tropical convection, *Clim. Dyn.*, *19*(15), 3445–3482.

Intergovernmental Panel on Climate Change (IPCC) (2007), *Climate Change 2007: The Physical Science Basis, Contribution of Working Group I to the Fourth Assessment Report of the Intergovernmental Panel on Climate Change*, edited by S. Solomon, et al., 996 pp., Cambridge Univ. Press, New York.

Krinner, G., et al. (2005), A dynamic global vegetation model for studies of the coupled atmosphere-biosphere system, *Global Biogeochem. Cycles*, *19*, GB1015, doi:10.1029/2003GB002199.

Labat, D., et al. (2004), Evidence for global runoff increase related to climate warming, *Adv. Water Res.*, *27*, 631–642.

Levis, S., R. A. Foley, and D. Pollard (2000), Large scale vegetation feedbacks on a double CO_2 climate, *J. Climate*, *13*, 1313–1325.

Liu, M. L., et al. (2008), Effects of land-use and land-cover change on evapotranspiration and water yield in china during 1900–2000, *J. Am. Water Resour. Assoc.*, *44*, 5, 1193–1207.

Madec, G., et al. (1998), OPA version 8.1 Ocean General Circulation Model, *Reference Manual, Note du Pôle de Modelisation, IPSL*, n°11, pp. 91, LODC, Université Paris VI, Paris 75252, France.

Marti, O., et al. (2010), Key features of the IPSL ocean atmosphere model and its sensitivity to atmospheric resolution, *Clim. Dyn.*, *34*, 1–26.

Milly, P. C. D., K. A. Dunne, and A. V. Vecchia (2005), Global pattern of trends in streamflow and water availability in changing climate, *Nature*, *438*, 347–350.

Peterson, B. J., et al. (2002), Increasing river discharge to the Arctic Ocean, *Science*, *298*, 2171–2173.

Piao, S., et al. (2007), Changes in climate and land use have a larger direct impact than rising CO_2 on global river runoff trends, *Proc. Natl Acad. Sci.*, *104*, 15,242–15,247.

Rayner, P. J., M. Scholze, and W. Knorr (2005), Two decades of terrestrial carbon fluxes from a carbon cycle data assimilation system (CCDAS), *Global Biogeochem.*, *19*(2), 2026–2028.

Stein, U., and P. Alpert (1993), Factor separation in numerical simulations, *J. Atmos. Sci.*, *50*, 2105–2115.

Sun, G., et al. (2008), Watershed evapotranspiration increased due to changes in vegetation composition and structure under a subtropical climate, *J. Am. Water Resour. Assoc.*, *44*(5), 1164–1175.

Twine, T. E., C. J. Kucharik, and J. A. Foley (2004), Effects of land cover change on the energy and water balance of the Mississippi River basin, *J. Hydrometeorol.*, *5*(4), 640–655.

Valcke, S., A. Caubel, R. Vogelsang, and D. Declat (2004), OASIS3 ocean atmosphere sea ice soil user's guide technical report TR/CMGC/04/68, CERFACS, Toulouse, France.

VanShaar, J. R., I. Haddeland, and D. P. Lettenmaier (2002), Effects of land-cover changes on the hydrological response of interior Columbia River basin forested catchments, *Hydrol. Processes*, *16*(13), 2499–2520.

R. Alkama, CNRS/Météo-France, GAME/CNRM, 42 ave. G. Coriolis, 31057 Toulouse, France. (ramdane.alkama@cnrm.meteo.fr)

M. Kageyama and G. Ramstein, Laboratoire des Sciences du Climat et de l'Environnement/IPSL UMR 8212 CEA, CNRS, l'Université de Versailles Saint-Quentin, 91191 Gif sur Yvette, France.